This is a repository copy of *Effect of calcium sulfates on the early hydration of calcium sulfoaluminate cement and the stability of embedded aluminium*.

White Rose Research Online URL for this paper:
http://eprints.whiterose.ac.uk/113982/

Version: Publishers draft (with formatting)

Proceedings Paper:
McCague, C, Bai, Y, Zhou, Q et al. (1 more author) (2014) Effect of calcium sulfates on the early hydration of calcium sulfoaluminate cement and the stability of embedded aluminium. In: NUWCEM 2014. Second International Symposium on Cement-Based Materials for Nuclear Wastes (NUWCEM2014), 03-06 Jun 2014, Avignon, France. , pp. 1-12.

Effect of calcium sulfates on the early hydration of calcium sulfoaluminate cement and the stability of embedded aluminium

C. McCague[1,2], Y. Bai[2*], Q. Zhou[2], P.A.M. Basheer[1]

[1] School of Planning, Architecture and Civil Engineering, Queen's University Belfast, U.K.

[2] Department of Civil, Environmental and Geomatic Engineering, University College London, U.K.

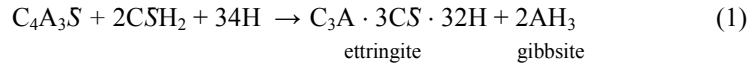*Corresponding author: yun.bai@ucl.ac.uk

Abstract Conventional Portland cement-based systems have been considered unsuitable for immobilising nuclear wastes containing reactive metals, such as aluminium, due to the high pH of the pore solution (usually around 12.5) and free moisture. On the contrary, calcium sulfoaluminate cement (CSA) produces a lower pH (10.5-12) environment and has an excellent water binding capability as a result of the formation of its main hydration product, ettringite. Therefore, it offers a good potential to immobilise aluminium. However, the pore solution pH and ettringite formation depend largely on the raw materials used to formulate the CSA, which is usually a blend of 75%-85% of CSA clinker and 15-25% of calcium sulfate (in the form of gypsum or anhydrite). In this paper, it was found that, compared to anhydrite, gypsum (15%wt of the blend) demonstrated the highest reduction in the corrosion of embedded Al, possibly due to its lower initial pH (around 10.5) and self-desiccating nature at the early stage of hydration. Whilst the CSA/anhydrite had a higher Al corrosion rate, the initial set was more acceptable than CSA/gypsum. Nonetheless, overall, it was concluded that CSA with gypsum (15%wt) should be considered as a base formulation for the encapsulation of Al waste. The unfavorable rapid set and high heat generation, however, demonstrated that modifications are required, potentially by using mineral additions.

1. Introduction

For the past few decades, Portland cement (PC) based systems have been used by the UK nuclear industry to immobilise many types of low and intermediate nuclear wastes. Compatible wastes are solidified in 500 litre stainless steel drums using a composite formulation, typically 10% PC with 90% blast furnace slag (BFS) [1]. The addition of BFS is necessary to reduce the high internal temperatures (and hence the stress) that can result from large pours. Nonetheless, since the opening

of the first cementation plant in the 1980s, studies have been ongoing to assess alternative options for dealing with incompatible legacy waste. Of these wastes, the most problematic are aluminium and uranium which corrode in the high pH/high moisture environment of conventional PC-based systems. Aluminium, for example, is only passive (i.e. no corrosion occurs) between pH 4 and 8.5.

Calcium sulfoaluminate cement (CSA) has been recognised as a potential alternative to PC, in particular, for immobilising aluminium [2]. In the presence of calcium sulfate and water, CSA clinker rapidly hydrates to form ettringite as the main hydration product. Unlike PC, calcium hydroxide is only produced in small amounts (from C_2S hydration, if C_2S is present) therefore the pH of the pore solution is considerably lower (values as low as 10.5 have been reported). Recent studies on CSA cement have demonstrated the effects of gypsum and anhydrite on cement hydration [3-5]. Gypsum for example, is a more reactive form of calcium sulfate and will rapidly react with CSA to form ettringite and gibbsite.

$$C_4A_3\bar{S} + 2C\bar{S}H_2 + 34H \rightarrow \underset{\text{ettringite}}{C_3A \cdot 3C\bar{S} \cdot 32H} + \underset{\text{gibbsite}}{2AH_3} \tag{1}$$

The use of gypsum may be desirable if rapid setting/strength development is required. However, this can lead to a higher heat output which is not desired for large pours (such as nuclear waste immobilisation). Anhydrite on the other hand, is less reactive, leading to longer setting times and better ettringite formation in the long-term [6].

$$C_4A_3\bar{S} + 2C\bar{S} + 38H \rightarrow C_3A \cdot 3C\bar{S} \cdot 32H + 2AH_3 \tag{2}$$
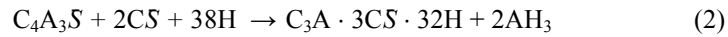
Without sulfate addition, CSA hydrates to form metastable calcium monosulfoaluminate (monosulfate) and gibbsite as the main hydration products [7].

$$C_4A_3\bar{S} + 18H \rightarrow \underset{\text{monosulfate}}{C_3A \cdot C\bar{S} \cdot 12H} + 2AH_3 \tag{3}$$
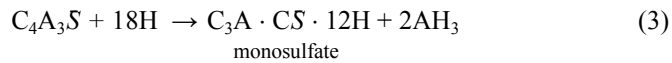
However, monosulfate could potentially convert to ettringite (in the presence of free sulfate ions), causing potential expansion at later ages. Therefore, careful consideration of the type and quantity of calcium sulfate is necessary to ensure maximum/stable ettringite formation, so to bind as much free water as possible.

Preliminary studies in the literature [8, 9] have demonstrated the potential of CSA for encapsulating nuclear wastes containing Al. The aim of this paper is to expand on a previous study by the authors [10], to investigate the corrosion performance of embedded aluminium metal in the CSA matrices formulated with different types of calcium sulfate (gypsum and anhydrite) in order to identify the most suitable formulation for immobilising nuclear wastes containing aluminium.

2.   Experimental

2.1. Materials

The CSA used for this study was 'Type II' CSA clinker (a CSA with coarser fineness) obtained from Hanson UK. This particular clinker consists of 71-75% ye'elimite ($C_4A_3\bar{S}$) and 14-18% belite (C_2S) as the main phases. Minor phases such as anhydrite ($C\bar{S}$), mayenite ($C_{12}A_7$) and perovskite (CaT) were also detected (Fig. 1). The coarser grain size of Type II (390 m^2/kg fineness) was expected to be less reactive, thus reducing heat output and prolonging setting times (a requirement for waste encapsulation) [1]. Gypsum powder (assay 99%) was obtained from Saint-Gobain UK and anhydrite powder (94% purity, 5% CaF$_2$, 0.5-2.0% CaO) was obtained from Francis Flower UK.
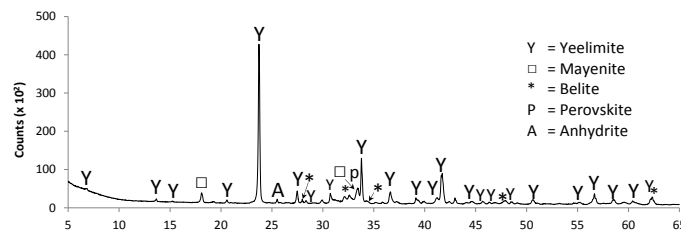

Fig. 1 X-ray diffractogram of Hanson CSA clinker

The aluminium metal used in this study was grade 1050A H14 (dimensions 50x30x5 mm) supplied by Aalco UK. This particular grade was chosen based on consultation with the UK nuclear industry [11]. For corrosion testing, a reference PC-based cement paste was prepared using PC (CEM1 42.5) with a high replacement (90%wt) with ground granulated blastfurnace slag (GGBS) at a water:solid (w/s) ratio of 0.5 (which gave a mini-slump of 80 ± 5 mm).

2.2. Test methods

2.2.1 Mini slump

The mini slump test can give a quick indication of the workability of fresh paste and is a useful tool for determining the minimum amount of water for achieving a desired workability. For the encapsulation of metals such as aluminium, the water content of any cement must be at a minimum. After consultation with industry [11], a mini slump value of 80 ± 5 mm was considered acceptable. Mini slump tests were carried out on CSA with 0, 15, 20, 25 and 30wt% of CSA replaced by

different types of calcium sulfate (with the mini slump measurement maintained at 80 ± 5 mm across all the samples).

2.2.2. Heat of hydration

To determine the optimum level of calcium sulfate, a calorimetry study was carried out on CSA formulations established through the mini slump tests. A multichannel (TA instruments) isothermal conduction calorimeter (ICC) was used to study the heat of hydration of the cement pastes at 20°C over a 5-day period.

2.2.3 Characterisation of cement pastes

The hydration products of each of the pastes were characterised using X-ray diffraction (XRD) analysis. Knowledge of the phase assemblage in the hydrated CSA pastes is necessary to understand the corrosion behavior of embedded aluminium.

2.2.4 pH measurement

The pH of the fresh and hardened pastes was measured using a double junction 'sleeve type' glass pH electrode (ROSS). For the fresh pastes, the electrode was inserted directly into the cement paste sample and monitored continuously before reaching initial set (Fig. 2). For the hardened pastes, a solution of 1 part hydrated cement (ground to 63microns) to 10 parts distilled water was prepared and stirred in a rotating stirrer for 24 hrs. The solid particles were separated from the solution using a centrifuge and the pH of the liquid containing the dissolved ions was then measured.

2.2.5 Corrosion testing

For this study, a tailored test cell was developed to house the cement-Al specimens for corrosion experiments (Fig. 3). A three-electrode configuration was adopted to facilitate the measurement of polarisation resistance, R_p. Using this parameter, the instantaneous corrosion rate of embedded aluminium could be calculated using the Stern-Geary relationship [12]. Aluminium 1050A H14 was used for both the working electrode (metal under study) and counter electrode (required to apply the polarising current), with a high grade stainless steel rod used as a solid-state reference electrode. A 'positive-feedback' compensating algorithm was built into every scan to compensate for the current-resistance (IR) drop induced by the ionic resistivity of the pastes. This was an improvement over the previous study where a correction for the cement resistance was not considered [9]. An embedded capacitance based RH/temperature sensor was also incorporated to provide complementary data to the corrosion rate measurements.

Fig. 2 pH measurement of fresh pastes   Fig. 3 Test setup for corrosion monitoring

3.   Results and discussion

3.1. Effect of calcium sulfates on fresh paste workability

The mini slump results are presented in Table 2. As can be seen, with 0% calcium sulfate added, the w/s ratio required to achieve the expected mini slump was 0.45. With gypsum additions, there was a slight decrease in the water demand compared to the pure CSA mix. However, with anhydrite, more water was required compared to the 0% mix. The stoichiometric w/s ratio for the hydration of CSA (after considering the impurities in the current CSA cement) can be as high as 0.6. Therefore, it is expected that using the w/s as shown in Table 2 would result in an undersupply of water during the hydration which could promote the self-desiccation of the hardened matrix. This would be advantageous for waste immobilisation, in particular, for the immobilisation of wastes containing Al as the reduced free water content would alleviate the corrosion of Al.

Table 2 Mini slump results

	100% CSA	CSA/gypsum				CSA/anhydrite			
CSA (wt%)	100	85	80	75	70	85	80	75	70
Gypsum (wt%)	−	15	20	25	30	−	−	−	−
Anhydrite (wt%)	−	−	−	−	−	15	20	25	30
Required w/s	0.45	0.43	0.43	0.43	0.44	0.46	0.46	0.45	0.5

3.2. Effect of calcium sulfates on CSA hydration

3.2.1.   Heat of hydration

The heat evolution during the hydration of each of the CSA/gypsum and CSA/anhydrite pastes is presented in Fig. 4 and Fig. 5 respectively. The pure CSA, i.e. 100% CSA, is denoted by 0% (i.e. with 0% of calcium sulfate). In all

6

pastes, there was a short heat event within the first hour which can be mainly attributed to the dissolution of anhydrous powders (peak I) [4]. Overall, when calcium sulfates (both gypsum and anhydrite) were added, only a slight reduction in the induction period of CSA hydration is observed [Figs. 4(a) and 5(a)]. Previous calorimetry studies by Winnefeld, however, demonstrated a much more significant reduction in the induction period after the addition of sulfate [3, 13]. In this study, it is likely that the small amount of anhydrite already in CSA clinker (as demonstrated in Fig. 1) allowed ettringite to form (peak II) thus corresponding to a fast induction period. In the 0% sample, the main heat event (peak III) has been attributed to the formation of monosulfate/CAH_{10} [3].
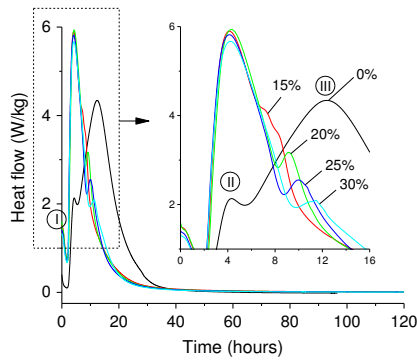

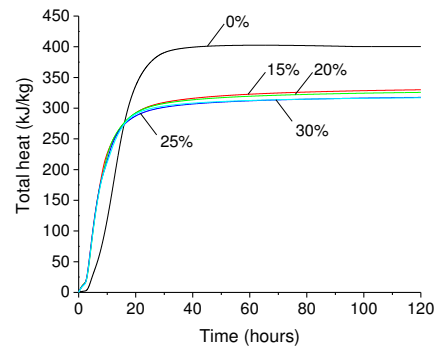Fig. 4 (a) Heat flow with gypsum
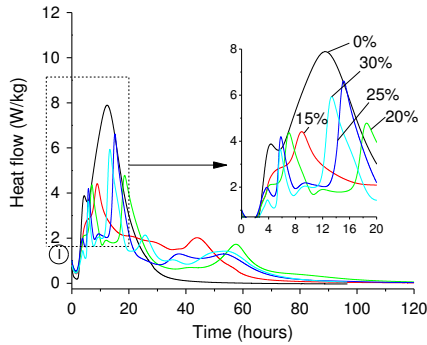
Fig. 4 (b) Total heat with gypsum
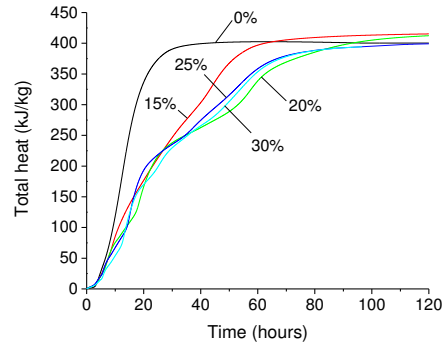

Fig. 5 (a) Heat flow with anhydrite

Fig. 5 (b) Total heat with anhydrite

When gypsum was used as a source of sulfate, its effect on the hydration of CSA can be clearly seen in Fig. 4. After the induction period, hydration was rapidly accelerated, reaching a maximum peak at 4 hrs. Similar to Chen's calorimetry study, changing the level of gypsum addition had little effect on the magnitude of peak II [4]. When gypsum was added at 15%, peak III appeared as a shoulder at ~6 hrs. As the level of gypsum was increased, the intensity of peak III decreased, shifting to later times (which has also been reported previously [3, 4]). As can be

seen from Fig. 5, the hydration kinetics of anhydrite is different from that of gypsum. Due to the lower reactivity of anhydrite, there was a decrease in the rate of ettringite formation from 0 to 4 hrs. Hydration is broken up into a series of peaks [as shown in Fig. 5(a)] which may be associated with the slow and steady dissolution of anhydrite [3].

As can be seen from Fig. 4(a), when the gypsum level increased above 15%, there is no obvious change to the shape of peak II which may indicate that 15% gypsum can be considered as the optimum level for the formation of ettringite [6]. Fresh paste pH trials revealed that, compared to 100% CSA (pH ~11.7), gypsum addition caused a significant reduction in initial pH (~10.5) whereas only a slight reduction was obtained with anhydrite (~11.7). Moreover, as calcium sulfate levels rose above 15%, there was no further change in initial pH (data not shown). Therefore, in the following study, 15% gypsum has been used. Nonetheless, pastes with 15% anhydrite were also studied in order to obtain further information on the effect of the sulfate source on both the hydration of CSA and the corrosion behaviour of embedded aluminium.

3.2.2. Phase analysis

The main phases detected by XRD are shown in Table 3. The 100% CSA, CSA/gypsum and CSA/anhydrite pastes are denoted by C1, C2 and C3 respectively. The AH_3 formed in CSA cements is amorphous, therefore, no XRD peaks were detected for AH_3 in all samples in the current study. However, the AH_3 was detected and quantified using thermogravimetry (data not presented in this paper). As indicated in Table 3, ettringite (denoted as AFt), CAH_{10} and monosulfate (denoted as AFm) were the main crystalline hydration products formed in C1 after 1day. The immediate ettringite formation was most likely a result of ye'elimite hydration with the anhydrite already present in the clinker (as presented in equation 2). It is possible that CAH_{10} was formed from the hydration of mayenite in the presence of insufficient sulfate ions whereby the formation of ettringite is less favored [14]. From the thermogravimetric analysis of C1 (data not shown), it was found that a decrease in AH_3 occurred between 2 and 7days. It is thus likely that some AH_3 reacted with C_2S to form strätlingite (S). This was also corroborated by the XRD traces obtained from a previous study where the main peaks for crystalline strätlingite emerged between 7 and 28days [15].

$$C_2S + AH_3 \rightarrow C_2ASH_8 \text{ (strätlingite)} \qquad (4)$$
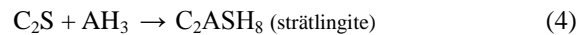
Similar to C1, CAH_{10} was detected in C3, however, began to develop later at 2days. It is likely that the slow dissolution of anhydrite led to an insufficient supply of sulfate ions and, hence, allowed the Ca^{2+} and $Al(OH)_4^-$ ions to dominate, which prevented the formation of ettringite from mayenite hydration [16]. In C2, on the other hand, it is likely that the rapid dissolution of gypsum enabled the sufficient supply of sulfate ions. As a result, the ettringite was formed at the expense of $CAH_{10.}$ As expected, ettringite was the main crystalline hydrate formed in C2

and C3. It is interesting to observe strong peaks for residual anhydrous phases present in both C2 and C3. Unlike C2, the peak intensities of most of the residual phases (except C_2S) in C3 almost diminished between 7 and 28days. It is worth mentioning that, although strätlingite was identified in C1 after 7 days, peaks for strätlingite were undetected in C2 and C3. This could be due to the reduced initial pH of C2 and C3 with pH of 10.4 and 11.4 being measured (see pH data in Fig.6) respectively as compared to that of C1 (pH 11.7), because according to Damidot and Glasser [17] strätlingite is unstable below ~pH 11.6. Nonetheless, in both cases of gypsum and anhydrite additions, the ettringite-rich matrices are expected to be able to reduce the corrosion rate of aluminium, particularly in the long term where aluminium corrosion rates are controlled by the supply of water and, hence, also by the ionic transport to the metal surface [18].

Table 3 Main crystalline phases detected by XRD

		$C_{12}A_7$	C_4A_3S	C_2S	CS	CSH_2	CAH_{10}	AFt	AFm	S
Clinker		■	■	■	□	−	−	−	−	−
C1	1d	−	■	■	−	−	■	■	■	−
	2d	−	■	■	−	−	■	■	■	−
	7d	−	■	■	−	−	■	■	■	□
	28d	−	■	■	−	−	■	■	■	■
C2	1d	−	■	■	−	■	−	■	□	−
	2d	−	■	■	−	■	−	■	□	−
	7d	−	■	■	−	■	−	■	−	−
	28d	−	■	■	−	■	−	■	−	−
C3	1d	−	■	■	■	−	−	■	−	−
	2d	−	■	■	■	−	□	■	−	−
	7d	−	□	■	□	−	■	■	−	−
	28d	−	□	■	□	−	■	■	−	−

■ = strong, □ = trace, − = absent

3.2.3. pH

The pH results are presented in Fig. 6. Measurements from the fresh and hardened pastes are separated by the dashed lines. The initial pH of C1 was measured as ~11.7. This pH is believed to be controlled by the dissolution of C_4A_3S (releasing alkalis) and aluminate phases present in the clinker [19]. At 4 hrs, the pH began to rise, gradually reaching a peak of 12.2 at 10.5 hrs. It is interesting to compare this to the ICC curve where the AFm peak occurred during the same period.

With the addition of gypsum to 100% CSA (C2), an immediate decrease in pH was observed, with a value as low as 10.4 being measured after 2.5 hrs. As shown in Fig. 6, pure gypsum paste (w/s 0.43) was measured as pH ~7.8. Therefore, the rapid dissolution of gypsum along with its lower pH would have led to this reduced pH compared to that measured from the C1. This would have enabled the ettringite to form at a rapid rate [20]. On the contrary, the pH of the pure anhydrite paste (w/s 0.45) was measured as ~12.3. However, it can be seen from Fig. 6 that the addition of anhydrite to 100% CSA (with a pH being measured as ~11.7), instead of increasing pH, has actually reduced the pH slightly at the early stage with

a pH value of 11.4 recorded at 4 hrs. This then began to stabilise at ~11.8 between 5 and 10 hrs. In the current study, it is still not clear why a reduction has been achieved. Further study is still needed to understand the interaction between CSA clinker and the anhydrite and its effect on the pore solution chemistry.

After 1 day, the pH of C1 slightly reduced compared to the final fresh paste measurement with a pH value of 11.97 recorded. However, in C2 and C3, a rise in pH occurred with 1-day values of 11.82 and 11.97 respectively. After 2 days, the pH of C3 decreased to 11.33 while C1 and C2 remained unchanged. From XRD, it was observed that better consumption of the anhydrous CSA clinker was achieved in C3 and, thus, could possibly have reduced the pH.
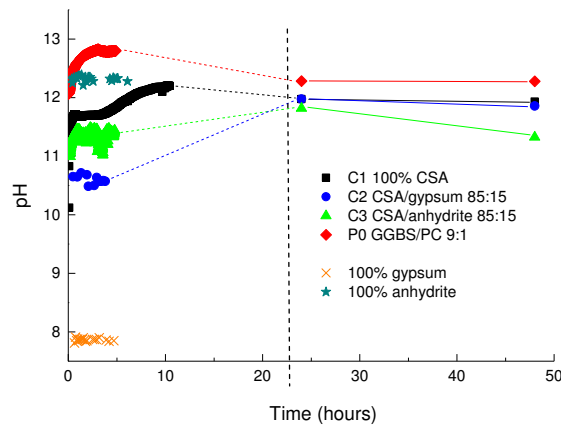


Fig. 6 pH of cement pastes up to 48 hrs

3.3. Effect of calcium sulfates on aluminium corrosion rate

Corrosion rates were calculated from IR-compensated R_p values using the Stern-Geary relationship [12]. Along with Al corrosion rates [Fig.7 (b)], the data from the embedded RH/temperature sensor is also displayed in Fig.7 (a).

In GGBS/PC 9:1 (P0), the corrosion of Al was almost immediate, rising rapidly to a peak rate of 1.56 mm/yr at 5.7 hrs. The high initial pH (~12.5) of the fresh paste causes the protective oxide layer to dissolve and the following anodic reaction takes place [18]:

$$Al \rightarrow Al^{3+} + 3e^- \tag{5}$$

Water is then reduced to hydroxyl and hydrogen gas at the cathode:

$$H_2O + 3e^- \rightarrow 3OH^- + 3/2H_2 \tag{6}$$
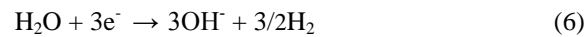
Combining the anodic and cathodic reactions gives:
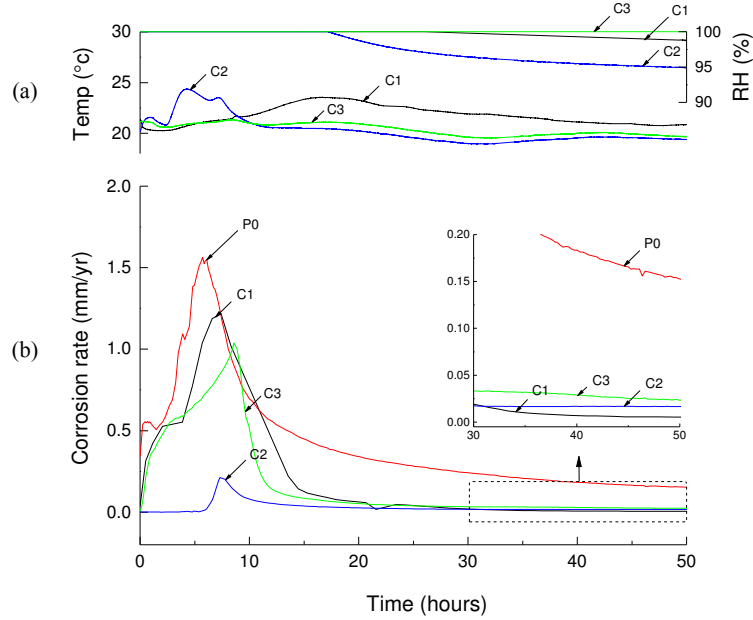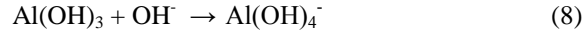
$$Al + 3H_2O \rightarrow Al(OH)_3 + 3/2H_2 \tag{7}$$
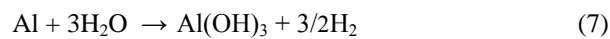
Fig. 7 (a) Internal RH and temperature (b) Corrosion rate of aluminium in CSA cements

It is likely that the increased alkalinity (~pH 12.8 at 3 hrs) led to the dissolution of the precipitated $Al(OH)_3$ formed in equation 7 through the following reaction:

$$Al(OH)_3 + OH^- \rightarrow Al(OH)_4^- \tag{8}$$

The instability of $Al(OH)_3$ prevents the formation of a protective corrosion layer therefore the corrosion of Al would remain active for longer periods.

In C1, Al corrosion was reduced compared to P0, with a peak of 1.22 mm/yr reached at 7.4 hrs. After ~10 hrs, a significant reduction in the corrosion rate occurred, decreasing to as low as 0.04 mm/yr after 1 day (compared to 0.3 mm/yr with P0). It is likely that the reduced pH and the high water binding capability of the hydration products of C1 (in this case both CAH_{10} and AFm) could have contributed to the 99% R.H. measured after 50 hrs and hence a reduction in the Al corrosion rate.

In C2, the early corrosion of Al was reduced even further, with corrosion almost non-existent over the 2day testing period. This can be attributed mainly to the lower initial pH resulting from gypsum addition. Even with a rise of internal temperature (peak of 28°C at 2.5 hrs), there was no active corrosion evident from the DC sweep analysis. On the other hand, the rapid formation of ettringite in C2 within the first few hours (as demonstrated by the ICC data in Fig.4) would result in a self-desiccating effect (R.H. 94% was measured after 2 days in [Fig. 7(a)]

with less free water available for corrosion.

In C3, the early corrosion of Al was reduced slightly compared to C1 with a peak rate of 1.03 mm/yr recorded at 8.5 hrs. This also correlates with the measurement of pH (Fig. 6) where only a slight reduction was measured compared to C1. From the calorimetry results, the addition of anhydrite was found to delay the initial setting therefore corrosion was allowed to continue for a greater period than C1 due to the availability of free moisture (as indicated in Fig. 7(a), 100% R. H. was measured even after 2 days).

Overall, from the results presented in Fig. 7, it can be concluded that C2 is the most suitable mix for immobilising aluminium due to its reduced pH and self-desiccation effect.

4.   Conclusions

In this paper, a hydration study of CSA using different types/levels of calcium sulfates was carried out in parallel with an aluminium corrosion study to assess the potential of CSA as a suitable alternative to PC for the encapsulation of aluminium.

Without additional sulfates, the fresh pH of CSA was found to be quite high with a value of 12.2 measured at 5 hrs. The peak corrosion rate of Al was therefore quite similar to the GGBS/PC control sample, however, a significant reduction occurred after ~10 hrs. With 15%wt gypsum blended with CSA, a significant reduction in Al corrosion performance was observed (effectively non-existant). This could be attributed to the lower initial pH (~10.4 and the rapid formation of ettringite (and hence the self-desiccation effect) as observed in the hydration study and R.H. measurement. With 15%wt anhydrite, the reduction of the early-age Al corrosion rate was less significant where only a slight decrease in peak corrosion rate was observed (compared to 100% CSA). It is understood that the lower dissolution rate of anhydrite had less of an impact on the chemical environment in CSA and therefore the effect on the pH was not as significant.

Overall, the pore solution pH was identified as the most significant factor affecting the early age Al corrosion in the cement pastes studied. In this respect, gypsum produced the more favorable conditions with the lowered initial pH. However, factors such as the phase assemblage/stability and RH are expected to be more critical at later ages.

12

5. References

1. Ojovan, M.I. and W.E. Lee, *Immobilisation of Radioactive Wastes in Cement*, in *An Introduction to Nuclear Waste Immobilisation*. 2005, Elsevier: Oxford. p. 189-200.
2. Milestone, N.B., *Reactions in cement encapsulated nuclear wastes: need for toolbox of different cement types.* Advances in Applied Ceramics, 2006. **105**(1): p. 13-20.
3. Winnefeld, F. and S. Barlag, *Influence of calcium sulfate and calcium hydroxide on the hydration of calcium sulfoaluminate clinker.* ZKG international, 2009. **62**(12): p. 42-53.
4. Chen, I.A. and M.C.G. Juenger, *Synthesis and hydration of calcium sulfoaluminate-belite cements with varied phase compositions.* Journal of Materials Science, 2011. **46**(8): p. 2568-2577.
5. Desbois, T., et al., *Effect of gypsum content on sulfoaluminate mortars stability.* European Journal of Environmental and Civil Engineering, 2010. **14**(5): p. 579-597.
6. Sahu, S., et al., *Hydration behaviour of sulphoaluminate belite cement in the presence of various calcium sulphates.* Thermochimica Acta, 1991. **175**(1): p. 45-52.
7. Hanic, F., I. Kaprálik, and A. Gabrisová, *Mechanism of hydration reactions in the system C4A3S-CS-CaO-H2O referred to hydration of sulphoaluminate cements.* Cement and Concrete Research, 1989. **19**(5): p. 671-682.
8. Zhou, Q., N.B. Milestone, and M. Hayes, *An alternative to Portland Cement for waste encapsulation--The calcium sulfoaluminate cement system.* Journal of Hazardous Materials, 2006. **136**(1): p. 120-129.
9. Hayes, M. and I.H. Godfrey, *Development of the use of alternative cements for the treatment of intermediate level waste*, in *Waste Management '07 Conference Tucson AZ*. 2007.
10. McCague, C., et al. *Early age corrosion of aluminium in calcium sulfoaluminate cement based composites*. in *NUWCEM 2011:1st International Symposium on Cement-based Materials for Nuclear Wastes*. 2011. Avignon, France.
11. Hayes, M. and N.C. Collier, *Email correspondance*. 2011.
12. Mansfeld, F., *The Polarization Resistance Technique for Measuring Corrosion Currents*, in *Advances in Corrosion Science and Technology*, M. Fontana and R. Staehle, Editors. 1976, Springer US. p. 163-262.
13. Winnefeld, F. and S. Barlag, *Calorimetric and thermogravimetric study on the influence of calcium sulfate on the hydration of ye'elimite.* Journal of Thermal Analysis and Calorimetry, 2010. **101**(3): p. 949-957.
14. Bayoux, A., et al., *Study of the hydration properties of aluminous cement and calcium sulfate mixes*, in *Calcium Aluminate Cements*, R.J. Mangabhai, Editor. 1990, Spon: London. p. 320-334.
15. Palou, M., et al., *Formation and stability of crystallohydrates in the non-equilibrium system during hydration of SAB cements.* Ceramics-Silikaty, 2005. **49**(4): p. 230-236.
16. Fu, X., et al., *Studies on effects of activators on properties and mechanism of hydration of sulphoaluminate cement.* Cement and Concrete Research, 2003. **33**(3): p. 317-324.
17. Damidot, D. and F.P. Glasser, *Investigation of the CaO-Al_2O_3-SiO_2-H_2O system at 25 °C by thermodynamic calculations.* Cement and Concrete Research, 1995. **25**(1): p. 22-28.
18. Armstrong, R.D. and V.J. Braham, *The mechanism of aluminium corrosion in alkaline solutions.* Corrosion Science, 1996. **38**(9): p. 1463-1471.
19. Andac, M. and F.P. Glasser, *Pore solution composition of calcium sulfoaluminate cement.* Advances in Cement Research, 1999. **11**(1): p. 23-26.
20. Havlica, J. and S. Sahu, *Mechanism of ettringite and monosulphate formation.* Cement and Concrete Research, 1992. **22**(4): p. 671-677.